

Influence of growth and annealing conditions on low-frequency magnetic 1/f noise in MgO magnetic tunnel junctions

Jiafeng Feng, Zhu Diao, Huseyin Kurt, Ryan Starrett, A. Singh, Edmund R. Nowak, and J. M. D. Coey

Citation: [Journal of Applied Physics](#) **112**, 093913 (2012); doi: 10.1063/1.4764314

View online: <http://dx.doi.org/10.1063/1.4764314>

View Table of Contents: <http://scitation.aip.org/content/aip/journal/jap/112/9?ver=pdfcov>

Published by the [AIP Publishing](#)

Articles you may be interested in

[Very low 1/f barrier noise in sputtered MgO magnetic tunnel junctions with high tunneling magnetoresistance](#)
J. Appl. Phys. **112**, 123907 (2012); 10.1063/1.4769805

[Improvement of the low-frequency sensitivity of MgO-based magnetic tunnel junctions by annealing](#)
J. Appl. Phys. **109**, 113917 (2011); 10.1063/1.3596817

[Magnetic noise evolution in CoFeB/MgO/CoFeB tunnel junctions during annealing](#)
Appl. Phys. Lett. **97**, 243502 (2010); 10.1063/1.3526721

[Low-frequency noise in MgO magnetic tunnel junctions](#)
J. Appl. Phys. **99**, 08T306 (2006); 10.1063/1.2165142

[Low-frequency noise and tunneling magnetoresistance in Fe \(110 \) MgO \(111 \) Fe \(110 \) epitaxial magnetic tunnel junctions](#)
Appl. Phys. Lett. **87**, 042501 (2005); 10.1063/1.2001128

High-Voltage Amplifiers

- Voltage Range from $\pm 50\text{V}$ to $\pm 60\text{kV}$
- Current to 25A

Electrostatic Voltmeters

- Contacting & Non-contacting
- Sensitive to 1mV
- Measure to 20kV



ENABLING RESEARCH AND
INNOVATION IN DIELECTRICS,
ELECTROSTATICS,
MATERIALS, PLASMAS AND PIEZOS



www.trekinc.com

TREK, INC. 190 Walnut Street, Lockport, NY 14094 USA • Toll Free in USA 1-800-FOR-TREK • (t):716-438-7555 • (f):716-201-1804 • sales@trekinc.com

Influence of growth and annealing conditions on low-frequency magnetic $1/f$ noise in MgO magnetic tunnel junctions

Jiafeng Feng,¹ Zhu Diao,¹ Huseyin Kurt,^{1,a)} Ryan Stearrett,² A. Singh,¹ Edmund R. Nowak,² and J. M. D. Coey¹

¹CRANN and School of Physics, Trinity College, Dublin 2, Ireland

²Department of Physics and Astronomy, University of Delaware, Newark, Delaware 19716, USA

(Received 30 July 2012; accepted 9 October 2012; published online 6 November 2012)

Magnetic $1/f$ noise is compared in magnetic tunnel junctions with electron-beam evaporated and sputtered MgO tunnel barriers in the annealing temperature range 350 - 425 °C. The variation of the magnetic noise parameter (α_{mag}) of the reference layer with annealing temperature mainly reflects the variation of the pinning effect of the exchange-bias layer. A reduction in α_{mag} with bias is associated with the bias dependence of the tunneling magnetoresistance. The related magnetic losses are parameterized by a phase lag ε , which is nearly independent of bias especially below 100 mV. The similar changes in magnetic noise with annealing temperature and barrier thickness for two types of MgO magnetic tunnel junctions indicate that the barrier layer quality does not affect the magnetic losses in the reference layer. © 2012 American Institute of Physics. [<http://dx.doi.org/10.1063/1.4764314>]

I. INTRODUCTION

The large tunneling magnetoresistance (TMR) in magnetic tunnel junctions (MTJs) with crystalline MgO barriers makes MgO-based MTJs potential candidates for applications as magnetic sensors with a high signal-to-noise ratio, provided the noise can be minimized. The large TMR is due to spin-dependent tunneling. Spin filtering by the MgO tunnel barrier is attributed to the absence of Bloch eigenstates in the minority \downarrow channel with Δ_1 symmetry at the Fermi level.¹⁻³ The electrodes are body-centred cubic $3d$ -ferromagnets and their alloys, such as Fe,⁴ Co,⁵ CoFe,⁶ and CoFeB.^{7,8} The MTJ stacks are usually grown by radio frequency sputtering with the MgO (001) tunnel barrier sandwiched between amorphous CoFeB electrodes,^{7,8} which are crystallized by subsequent annealing. Recently, our group found that electron-beam (EB) evaporation is an alternative method for growing good MgO in MTJs. A TMR value of 240% has been achieved at room temperature in exchange-biased EB-MgO MTJs.⁹ Furthermore, a low level of barrier noise is observed due to the low density of oxygen vacancies in EB-MgO.¹⁰ This noise level is comparable to that in junctions where the MgO is grown by molecular beam epitaxy.¹¹

Noise spectra of MTJ sensors are usually dominated by $1/f$ noise in the low-frequency range, which can be either magnetic or electronic (nonmagnetic) in origin.^{12,13} We distinguish the electronic noise of the barrier from the noise due to magnetic fluctuations in the ferromagnetic layers. Electronic $1/f$ noise is a spin-independent resistance fluctuation¹⁴ due, for example, to localized charge traps.^{10,15,16} It is associated with the tunnel barrier and it is related to the barrier growth method and the annealing treatment.^{10,11,17} Magnetic $1/f$ noise is the performance-limiting factor in MTJ sensors.^{13,18} It originates from thermally activated fluctuations of

the magnetization of the ferromagnetic layers, and it can be related to the magnetic susceptibility through the fluctuation-dissipation theorem.^{19,20} The magnetic noise is usually expressed by a Hooge-like parameter, $\alpha_{\text{mag}} = S_V^{\text{mag}} f \Omega / V^2$,²⁰ where S_V^{mag} is the voltage noise power spectral density due to magnetic fluctuations, f is the frequency, Ω is the volume of the ferromagnetic layer, and V is the voltage applied to the MTJ. To obtain S_V^{mag} , the amplifier noise, thermal and shot noise, and the electronic $1/f$ noise arising from the tunnel barrier have to be subtracted from the measured noise power spectral density S_V . The quantity α_{mag} allows one to compare the magnetic noise level in different magnetic states for different MTJs. It has also been shown that α_{mag} is proportional to the magnetoresistance-sensitivity product, $\text{MSP} \equiv (\Delta R / R^2)(dR/dH)$, in a MR sensor, and follows the relation:²⁰

$$\alpha_{\text{mag}} \approx \varepsilon(H) \frac{k_B T}{\pi \mu_0 M_s} \frac{\Delta R}{R} \left(\frac{1}{R} \frac{dR}{dH} \right), \quad (1)$$

where ΔR is the total resistance change between the parallel (P) and antiparallel (AP) states, $\mu_0 M_s$ is the saturation magnetization of magnetic electrodes (1.6 T for $\text{Co}_{40}\text{Fe}_{40}\text{B}_{20}$), k_B is Boltzmann's constant, T is the absolute temperature in Kelvin, and μ_0 is the permeability of free space ($4\pi \times 10^{-7}$ T m A⁻¹). The phase lag $\varepsilon(H)$ is the ratio of the imaginary and real parts of the ac resistance susceptibility χ_R''/χ_R' , providing $\chi_R'' \ll \chi_R'$. It may be directly measured by monitoring the response of the device to a small ac magnetic field,¹⁹⁻²¹ or estimated from the slope of the α_{mag} versus MSP relation, following Eq. (1),^{20,21} where α_{mag} and MSP are extracted from the noise and resistance versus magnetic field curves, respectively.

Recently, Ozbay *et al.*²⁰ investigated the magnetic $1/f$ noise in giant magnetoresistance and MTJ spin valves, and compared magnetic losses in their free and reference ferromagnetic layers. Stearrett *et al.*²² further studied the influence

^{a)}Present address: Engineering Physics Department, Istanbul Medeniyet University, Goztepe Kadikoy, Istanbul, Turkey.

of annealing on magnetic noise and losses in sputtered MgO-barrier MTJs. Magnetic losses in the reference layer started to decrease after prolonged thermal annealing, which was attributed to reduced magnetic disorder. In a separate report, Stearrett *et al.*²³ observed an influence of the exchange bias coupling on the magnetic losses in MgO-based MTJs through variation in the seed layer thickness and annealing treatment. Thicker seed layers induced more magnetic disorder and greater exchange bias, while prolonged annealing had the opposite effect.

In this work, we compare the magnetic $1/f$ noise in both EB- and sputtered (S-) MgO MTJs with different barrier thicknesses as a function of the annealing temperature T_a , for a fixed annealing time of 1 h. We focus on the magnetic noise during the reference layer magnetization switching, where a noise peak appears in the noise versus magnetic field loop. It is found that the magnetic noise is not greatly altered by post-deposition annealing in the range $350 < T_a < 425$ °C, used to crystallize CoFeB at the interfaces. The bias dependence of the magnetic noise and losses is also investigated. Though the barrier noise in two kinds of MTJs is very different,¹⁰ due to the difference in barrier quality, we demonstrate that the magnetic losses in the reference layer are not affected.

II. EXPERIMENTS

We fabricated exchange-biased EB-MgO MTJs with MgO layer thicknesses $t = 1.5, 2.0,$ and 2.5 nm,⁹ which makes it possible to investigate the barrier thickness dependence of the magnetic noise. The bottom pinned MTJ stacks were composed of the following layers:

Ta 5/Ru 30/Ta 5/Ni₈₁Fe₁₉ 5/Ir₂₂Mn₇₈ 10/Co₉₀Fe₁₀ 2.5/Ru 0.9/Co₄₀Fe₄₀B₂₀ (CoFeB) 3/MgO t /CoFeB 3/Ta 5/Ru 10, where the layer thicknesses are given in nm. The active part of the MTJ stack (CoFeB/EB-MgO/CoFeB) was deposited in the ultra-high-vacuum chamber of our Shamrock sputtering tool where the base pressure is 2.1×10^{-10} Torr. The other metallic layers were deposited by dc-magnetron sputtering in a separate high-vacuum chamber of the Shamrock system. For comparison, $t = 1.8, 2.0,$ and 2.4 nm S-MgO MTJs with CoFeB electrodes were also fabricated. The ferromagnetic electrodes for both types of MTJs were grown in similar conditions, such as argon pressure, growth rate, and composition of the CoFeB electrodes. High-vacuum post-deposition annealing of the devices was performed in a magnetic field of 800 mT. We refer to our earlier work on MgO MTJs for details related to their growth, transport properties, and structural characterization.^{9,10,24}

III. RESULTS AND DISCUSSION

Figure 1 shows junction resistance and low-frequency noise in an octave centered at 4.8 Hz normalized over the reference layer volume, measured simultaneously under a constant bias current ($5 \mu\text{A}$) for an EB-MgO MTJ. H_Λ denotes the field point at which magnetic noise power exhibits a broad maximum during the reference layer switching, which is normally close to the exchange bias field (H_{ex} , see Fig. 1) deduced from the magnetization curve. H_{ex} can be used to

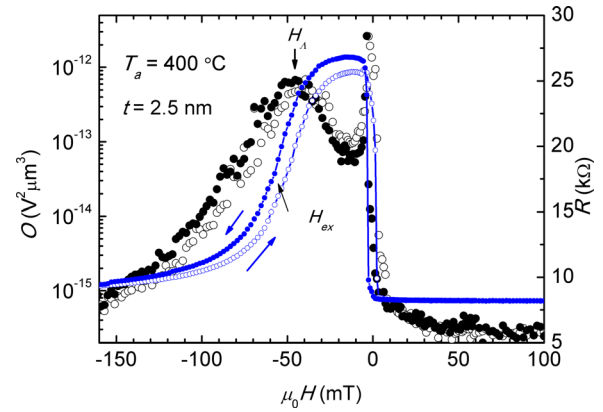


FIG. 1. Magnetic field dependence of the noise power spectrum in an octave centered at 4.8 Hz normalized over the reference layer volume and the magnetoresistance curve for an EB-MTJ with $t = 2.5$ nm at $I = 5 \mu\text{A}$. The noise and resistance were measured simultaneously.

quantify the pinning effect induced by the IrMn layer. The magnetic noise peaks at H_Λ are different when measured for increasing and decreasing magnetic field in these MTJs, and the magnitude of two noise peaks becomes more asymmetric with decreasing the barrier thickness. Because the MTJ structures in our work are similar to those in Ref. 25, the increase in asymmetry with decreasing the barrier thickness may be due to the increase of the interlayer magnetic coupling across the barrier (see the discussion below). We use the higher noise peak at H_Λ measured in the increasing field direction for our noise data analysis.

We have previously found that there is no great difference in the TMR ratio for EB-MTJs with either 2.0 or 2.5 nm MgO for any T_a .⁹ Since values for α_{mag} and MSP are comparable for MgO MTJs having resistance-area products in the range of $1 \text{ k}\Omega \mu\text{m}^2 - 1 \text{ M}\Omega \mu\text{m}^2$, here, we report data on EB-MTJs having $t = 1.5$ and 2.5 nm, as shown in Fig. 2. Both α_{mag} and MSP show a similar change with annealing temperature; they increase initially²² and then decrease. The increase

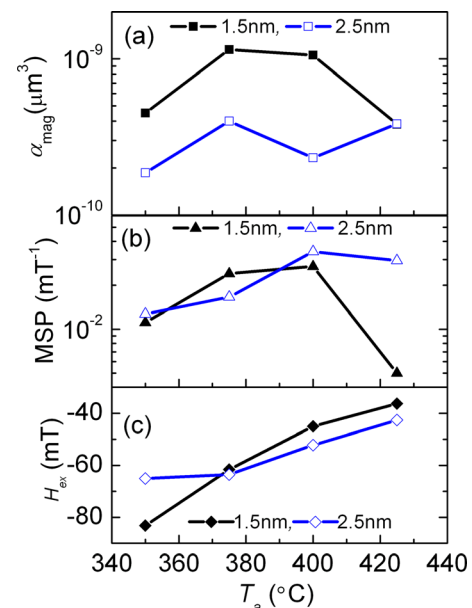


FIG. 2. Annealing temperature dependence of α_{mag} (a) and MSP (b), and H_{ex} (c) for the reference layer of EB-MgO MTJs with $t = 1.5$ and 2.5 nm.

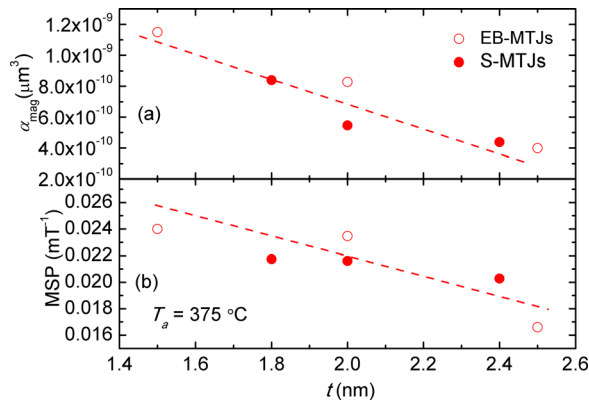


FIG. 3. The barrier thickness dependence of α_{mag} (a) and MSP (b) for both types of MTJs. Dashed lines are guides to the eye.

in α_{mag} and MSP with T_a may be mainly due to the degradation of the pinning effect; see Fig. 2(c), but these quantities decrease again at 425°C when the pinning is nearly destroyed. This behavior is similar to that shown in Fig. 4(d) of Ref. 9. Besides, α_{mag} is somewhat higher for $t = 1.5$ nm than for $t = 2.5$ nm. The interlayer magnetic coupling across the barrier is known to be dominated by the Néel “Orange Peel” interactions due to interface roughness provided the barrier thickness is more than 1.0 nm.²⁶ Hence, this difference in magnetic noise between $t = 1.5$ and 2.5 nm samples may come from the MgO/CoFeB interfaces. The thinner MgO layer is believed to have more interface roughness, which may lead to stronger interlayer dipole coupling. More coupling results in higher α_{mag} . Moreover, since the MgO (001) layer serves as a template for the crystallization of both top and bottom CoFeB electrodes during the post-deposition anneal, a thicker barrier may serve as a better template for crystallization than a thinner one. Less magnetic noise occurs in MTJs with thicker MgO layers. This observation is further demonstrated by the data in Figs. 3(a) and 3(b) for both EB- and S-MTJs, taken at a bias voltage $V = 50 - 80$ mV where α_{mag} and MSP remain constant in this voltage range. Both α_{mag} and MSP are nearly the same in magnitude for both EB- and S-MTJs and follow the same dependence on barrier thickness.

Following Eq. (1), we plot $\mu_0 M_s \alpha_{\text{mag}}$ as a function of MSP for EB-MTJs in Fig. 4(a). Data shown are summarized for samples annealed at 375 and 400°C . Higher ε is obtained for $t = 1.5$ nm, and the reason has been discussed above. Despite a large difference in their respective resistance-area products due to the MgO thickness difference, ε is similar for all the samples with the same MgO thickness, which changes a little with T_a . This is not surprising as ε is a property of the ferromagnetic layer, defined mainly by its growth conditions. For instance, the thin Ru layer below the reference layer in the synthetic antiferromagnetic (SAF) pinned stack may influence the magnetic losses.^{23,27} For these EB- and S-MgO MTJs, their antiferromagnetic layer and SAF layers are the same, which may lead to a similar level of magnetic disorder in the reference layer.

This is further illustrated by Fig. 4(b), where $\mu_0 M_s \alpha_{\text{mag}}$ during the reference layer switching is shown as a function of MSP for an EB-MTJ. Data points (blue open squares) are

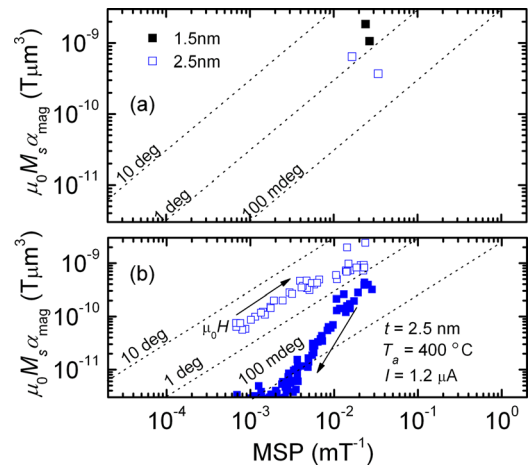


FIG. 4. (a) Plot of $\mu_0 M_s \alpha_{\text{mag}}$ as a function of MSP for EB-MgO MTJs with $t = 1.5$ and 2.5 nm, taken at $T_a = 375$ and 400°C ; and (b) the MSP dependence of $\mu_0 M_s \alpha_{\text{mag}}$ for an EB-MgO MTJ with $t = 2.5$ nm at $T_a = 400^\circ\text{C}$.

taken in a field range from -13 mT to -55 mT (close to H_Λ and $H_{c\lambda}$). The relation between $\mu_0 M_s \alpha_{\text{mag}}$ and MSP is linear, as predicted by Eq. (1), and previously reported in sputtered MgO MTJs.^{20,22} This linear relation suggests that the ε value is nearly constant in a large field range before the magnetization switching of the reference layer. However, a clear field dependence of ε occurs after the reference layer magnetization switching, see data points (blue filled squares) shown in Fig. 4(b), taken for $-57 > \mu_0 H > -200$ mT. The change of ε during the magnetization reversal of the reference layer has been previously reported.²³ It is obvious that the magnetic losses can be reduced when the pinning is weaker. As a result, the magnetic losses of the top-pinned CoFeB electrode in S-MTJ sensor devices decrease after inserting a thin Ru layer between CoFeB and IrMn; accordingly ε changes from $\sim 0.8^\circ$ for direct pinning to $\sim 0.1^\circ$ when the pinning becomes weaker.²⁷

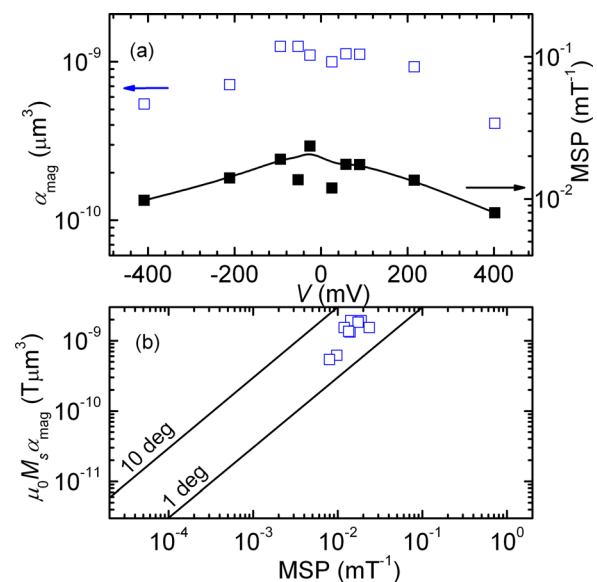


FIG. 5. (a) Bias dependence of α_{mag} and MSP, and (b) $\mu_0 M_s \alpha_{\text{mag}}$ as a function of MSP at different bias for an EB-MTJ with $t = 2.5$ nm and $T_a = 400^\circ\text{C}$. The black line in (a) is a guide to the eye.

Finally, another interesting observation in the present study comes from the bias dependence of magnetic noise and losses. There has been a number of reports^{28–30} of a reduction in the normalized noise parameter as a function of bias in MTJs in the AP state. The variation of normalized noise parameter in the AP state with bias was previously compared to the TMR - bias variation.¹¹ However, little explanation of this behavior has been given to date. Figure 5(a) shows the bias dependence of α_{mag} of the reference layer taken at H_{Λ} . α_{mag} is almost unchanged at low bias, but it starts to decrease at high bias. Compared to α_{mag} , MSP shows a similar change with bias, as indicated by black filled squares in Fig. 5(a). In Fig. 5(b), we collect data on ε under different bias in a $\mu_0 M_s \alpha_{\text{mag}}$ - MSP plot. A diagonal line (if drawn) passes through most of the data points indicating that ε remains fairly constant, particularly at low bias. The decrease of α_{mag} with bias may be attributed mainly to a decrease of MSP (see the case shown in Fig. 5(a)). A reduced TMR ratio couples into MSP in Eq. (1), which eventually leads to a reduced α_{mag} .

IV. CONCLUSION

The comparison of the magnetic noise of the reference layer for both EB- and S-MgO MTJs leads to the following conclusions. With the increase of annealing temperature, both α_{mag} and MSP increase gradually before they become stable or fall off due to the loss of the pinning effect. The phase lag ε in the ferromagnetic layers is relatively stable under annealing for a fixed time and its contribution to the magnetic $1/f$ noise cannot be reduced much by selecting an optimized bias voltage. There is almost no difference for magnetic noise and losses for MTJs with MgO barriers grown by electron-beam evaporation and sputtering. The challenge in realizing MTJ magnetic field sensors having a high signal-to-noise ratio involves reducing the magnetic loss term, while keeping the MSP high.

ACKNOWLEDGMENTS

This work was supported by SFI as part of the NISE Project, Contract 10/IN1.13006 and was conducted under the framework of the INSPIRE Program, funded by the Irish Government's Program for Research in Third Level Institutions, Cycle 4, National Development Plan 2007–2013. Some data analysis was performed at Delaware and was supported by DOE under Award DE-FG02-07ER46374. R. S. was supported by a NASA Space Grant Fellowship.

- ¹W. H. Butler, X.-G. Zhang, T. C. Schulthess, and J. M. MacLaren, *Phys. Rev. B* **63**, 054416 (2001).
- ²J. Mathon and A. Umerski, *Phys. Rev. B* **63**, 220403 (2001).
- ³X.-G. Zhang and W. H. Butler, *Phys. Rev. B* **70**, 172407 (2004).
- ⁴S. Yuasa, A. Fukushima, T. Nagahama, K. Ando, and Y. Suzuki, *Nature Mater.* **3**, 868 (2004).
- ⁵S. Yuasa, A. Fukushima, H. i. Kubota, Y. Suzuki, and K. Ando, *Appl. Phys. Lett.* **89**, 042505 (2006).
- ⁶S. S. P. Parkin, C. Kaiser, A. Panchula, P. M. Rice, B. Hughes, M. Samant, and S. H. Yang, *Nature Mater.* **3**, 862 (2004).
- ⁷Y. M. Lee, J. Hayakawa, S. Ikeda, F. Matsukura, and H. Ohno, *Appl. Phys. Lett.* **89**, 042506 (2006).
- ⁸S. Ikeda, J. Hayakawa, Y. Ashizawa, Y. M. Lee, K. Miura, H. Hasegawa, M. Tsunoda, F. Matsukura, and H. Ohno, *Appl. Phys. Lett.* **93**, 082508 (2008).
- ⁹H. Kurt, K. Oguz, T. Niizeki, and J. M. D. Coey, *J. Appl. Phys.* **107**, 083920 (2010).
- ¹⁰Z. Diao, J. F. Feng, H. Kurt, G. Feng, and J. M. D. Coey, *Appl. Phys. Lett.* **96**, 202506 (2010).
- ¹¹F. G. Aliev, R. Guerrero, D. Herranz, R. Villar, F. Greullet, C. Tiusan, and M. Hehn, *Appl. Phys. Lett.* **91**, 232504 (2007).
- ¹²J. M. Almeida, R. Ferreira, P. P. Freitas, J. Langer, B. Ocker, and W. Maass, *J. Appl. Phys.* **99**, 08B314 (2006).
- ¹³W. F. Egelhoff, Jr., P. W. T. Pong, J. Unguris, R. D. McMichael, E. R. Nowak, A. S. Edelstein, J. E. Bumette, and G. A. Fischer, *Sens. Actuators, A* **155**, 217 (2009).
- ¹⁴D. Reed, C. Nordman, and J. Daughtoon, *IEEE Trans. Magn.* **37**, 2028 (2001).
- ¹⁵J. Scola, H. Polovy, C. Fermon, M. Pannetier-Lecoecq, G. Feng, K. Fahy, and J. M. D. Coey, *Appl. Phys. Lett.* **90**, 252501 (2007).
- ¹⁶E. R. Nowak, M. B. Weissman, and S. S. P. Parkin, *Appl. Phys. Lett.* **74**, 600 (1999).
- ¹⁷R. Stearrett, W. G. Wang, L. R. Shah, A. Gokce, J. Q. Xiao, and E. R. Nowak, *J. Appl. Phys.* **107**, 064502 (2010).
- ¹⁸P. P. Freitas, R. Ferreira, S. Cardoso, and F. Cardoso, *J. Phys.: Condens. Matter* **19**, 165221 (2007).
- ¹⁹H. T. Hardner, M. B. Weissman, M. B. Salamon, and S. S. P. Parkin, *Phys. Rev. B* **48**, 16156 (1993).
- ²⁰A. Ozbay, A. Gokce, T. Flanagan, R. A. Stearrett, E. R. Nowak, and C. Nordman, *Appl. Phys. Lett.* **94**, 202506 (2009).
- ²¹N. Smith, A. M. Zeltser, D. L. Yang, and P. V. Koepe, *IEEE Trans. Magn.* **33**, 3385 (1997).
- ²²R. Stearrett, W. G. Wang, L. R. Shah, J. Q. Xiao, and E. R. Nowak, *Appl. Phys. Lett.* **97**, 243502 (2010).
- ²³R. Stearrett, W. G. Wang, X. M. Kou, J. F. Feng, J. M. D. Coey, J. Q. Xiao, and E. R. Nowak, *Phys. Rev. B* **86**, 014415 (2012).
- ²⁴H. Kurt, K. Rode, K. Oguz, M. Boese, C. C. Faulkner, and J. M. D. Coey, *Appl. Phys. Lett.* **96**, 262501 (2010).
- ²⁵J. F. Sierra, F. G. Aliev, R. Heindl, S. E. Russek, and W. H. Rippard, *Appl. Phys. Lett.* **94**, 012506 (2009).
- ²⁶J. Faure-Vincent, C. Tiusan, C. Bellouard, E. Popova, M. Hehn, F. Montaigne, and A. Schuhl, *Phys. Rev. Lett.* **89**, 107206 (2002).
- ²⁷J. Y. Chen, J. F. Feng, and J. M. D. Coey, *Appl. Phys. Lett.* **100**, 142407 (2012).
- ²⁸J. F. Feng, Z. Diao, and J. M. D. Coey, *J. Phys.: Conf. Ser.* **303**, 012098 (2011).
- ²⁹J. M. Almeida, P. Wisniewski, and P. P. Freitas, *IEEE Trans. Magn.* **44**, 2569 (2008).
- ³⁰A. Gokce, E. R. Nowak, S. H. Yang, and S. S. P. Parkin, *J. Appl. Phys.* **99**, 08A906 (2006).